

MALAYSIAN JOURNAL OF ANALYTICAL SCIENCES



Journal homepage: https://mjas.analis.com.my/

Research Article

Turning waste into fuel: Hydrodeoxygenation of sewer grease into hydrocarbon fuel via Fe foam modified catalyst

Muhammad Hasif Auji Fadzli¹, Nurul Asikin-Mijan^{1*}, Ghassan Kareem-Alsultan^{2,3**}, Darfizi Derawi¹, Yun Hin Taufiq-Yap^{2,3}, Hwei Voon Lee⁴, Karen Wilson⁵, Salman Raza Naqvi⁶, Salma Samidin⁷, Muhammad Rahimi Yusop¹, and Faris Ali Jassim Aldoghachi⁸

¹Department of Chemical Sciences, Faculty of Science and Technology, Universiti Kebangsaan Malaysia, 43600 UKM Bangi, Selangor Darul Ehsan, Malaysia

²Catalysis Science and Technology Research Centre, Faculty of Science, Universiti Putra Malaysia, 43400 UPM Serdang, Selangor, Malaysia

³Department of Chemistry, Faculty of Science, Universiti Putra Malaysia, 43400 UPM Serdang, Selangor, Malaysia

⁴Nanotechnology and Catalysis Research Centre (NanoCat), Institute of Postgraduate Studies, University Malaya, 50603 Kuala Lumpur, Malaysia

⁵School of Environment & Science, Centre for Catalysis and Clean Energy, Griffith University, Gold Coast Campus, QLD 4222, Australia

⁶Department of Engineering and Chemical Sciences, Karlstad University, Karlstad, Sweden

⁷Department of Chemical and Process Engineering, Faculty of Engineering and Built Environment, Universiti Kebangsaan Malaysia, 43600 UKM Bangi, Selangor, Malaysia

⁸Chemistry Department, Faculty of Science, University of Basrah, 61004, Basrah, Iraq

*Corresponding author: nurul.asikin@ukm.edu.my, kreem.alsultan@yahoo.com

Received: 19 September 2024; Revised: 20 July 2025; Accepted: 23 July 2025; Published: 22 August 2025

Abstract

Green diesel is an alternative petroleum derived fuel owing to their non-renewable nature and high CO_2 emissions. Hence, the present study highlights the production of green diesel from renewable and cost-effective fat, oil, and grease (FOG) via hydrodeoxygenation (HDO) reaction over a bimetallic-modified catalyst known as Ni_aCe_b/Fe -F using a series of Ce loadings ($Ni_{0.34}Ce_{0.30}/Fe$ -F, $Ni_{0.34}Ce_{0.42}/Fe$ -F) which were synthesized via the electrodeposition method. Detailed catalyst characterization was conducted, and most of the catalysts exhibited surface areas within the range of 4.45-45.13 m²/g, with 76-233 μ molg⁻¹ of acid sites. The presence of cerium species not only amplifies the number of acid sites but also facilitates the efficient removal of oxygen species, marking a pivotal advancement in the process. The catalyst also demonstrated a significant needle-like morphological structure. Based on the catalytic HDO screening study at 400 °C within a 6 h reaction time, the $Ni_{0.34}Ce_{0.42}/Fe$ -F (rich Ce vacancy species) catalytic HDO was found to be superior in catalytic activity compared to other catalysts, with a hydrocarbon yield of 53% and selectivity of 74% n-(C₁₅-C₁₈). Despite having a low surface area, the presence of high weak + medium acid sites in the catalyst, helped boost its catalytic activity in HDO.

Keywords: green diesel, cerium, hydrodeoxygenation, iron, nickel

Introduction

With the population increase and economic growth at a rapid rate, particularly in the urban areas of developing countries, energy consumption and demand have grown tremendously. Hence, resulting in an increase in the demand for fossil fuels worldwide. According to the International Energy Agency (IEA), primary energy demand worldwide rose by 2% [1]. As petroleum fuels release CO₂ when they are burned,

intensified energy use has led to over 40 gigatonnes of CO₂ emission in 2023 across the globe [2]. Actually, it leads to enormous issues like environmental contamination, greenhouse gas emission, and climatic alteration. Therefore, to curb this environmental problem, the quest for clean and sustainable energy as a substitute for fossil fuels is essential in curbing environmental degradation and providing a sustained energy supply. Over the past few years, many studies

have been carried out in investigating the possibilities of renewable diesel replacing petroleum diesel as the main source of energy in the future.

In recent years, numerous studies have been conducted in the search for the potential of renewable diesel to replace petroleum diesel as the primary source of energy in the future. Green diesel or "renewable diesel" is a promising substitute for conventional diesel fuel [3]. Green diesel produced from primarily agricultural waste such as organic oil, animal fats, and greases [4-6], which can be extracted in a process known as hydro-treatment of fatty acids or vegetable oil [4]. Sewer grease, or fats, oils, and grease (FOG), is waste material that comes primarily from the food industry (food preparation and food processing) and residential homes, such as cooking meat fat, lard, butter, and used cooking oil [7]. FOG has been a serious environmental problem because FOG settling can cause sewer pipe clogging, sewer overflows, and water pollution because it solidifies [8,9]. For solving this issue, recent research has demonstrated the potential of sewer grease as a feedstock for the production of green diesel [10,11]. Since FOGs are comprised of a high concentration of lipids from animal fat and vegetable oils It has been suggested as a promising green diesel feedstock that circumvents many economic constraints, such as its cost-effectiveness, and is available in bulk quantities because it does not compete with the human food chain [12,13]. FOG-derived green diesel possesses better characteristics compared to other feedstocks with respect to oxidative stability, flash point, cetane number, and total emissions [11]. Thus, the application of FOG in green diesel is beneficial in various ways. First, it addresses the issue of the environment by reducing disposal need and clogging of sewers. Second, it is a low-cost and renewable source of fuel.

possible catalytic diesel is bv hydrodeoxygenation (HDO) of the triglycerides [14]. HDO is highly carbon-efficient with an efficiency of approximately 100% since all the carbon is converted into hydrocarbons without emitting CO₂ [15]. Observed, the majority of the earlier research used powder catalysts in HDO reactions [16,17]. However, this powder catalyst possesses some serious drawbacks like severe flow blockage, uncontrollable liquid dynamics, and formation of hot spots. The mass transfer limitation usually depends a great deal on the flow conditions like pressure, temperature, surface velocity within the reactor, and catalyst structure [18]. Choice of catalysts for HDO depends on the acidic sites, high surface area, porosity, and stability of the catalysts. Although the surface area of the catalyst has been reported to accelerate the activity of HDO, recent studies have shown the critical roles played by catalyst acidic sites during the HDO process and hinted that the sites are more critical than surface area in regulating catalytic activity [19-22]. In addition, HDO also has superior oxygen vacancy sites. For instance, according to research supported by data from XPS obtained, Ni/Ti1Zr4 contained more oxygen vacancy sites than others and hence facilitated the adsorption of anisole and thus possessed superior HDO activity [23–26]. Based on the above findings, in this study, a highly stable, porous catalyst with high weakly acidic and defect sites will be engineered to catalyse the HDO of sewer grease to FOG-green diesel. Large porous, acidic, and oxygen vacancyabundant sites will be generated here by electrodepositing an oxygen-vacancy-rich bimetallic NiCe nanosheet of varying thicknesses onto a porous 3D Fe Foam. The porous nanosheet open cellular structure of the 3D Fe Foam has a much larger surface area, allowing for better mass transfer. Moreover, the nickel (Ni) and cerium (Ce) deposition over the porous nanosheet enables improved chemical and mechanical stability of the catalyst, which is then more efficient for the HDO process.

Materials and Methods Materials

The experiment began with the acquisition of Fe Foam (Fe-F) from a supplier. Meanwhile, high-purity chemicals, including nickel (II) nitrate hexahydrate (with a purity of over 99.0%) and cerium (IV) sulfate (with a purity exceeding 99.9%), were obtained from Sigma-Aldrich Pty Ltd., Malaysia. Additionally, Chemiz Malaysia provided analytical grade reagents, including hydrochloric acid (37%) and potassium hydroxide (KOH). Chemiz Malaysia also supplied solvents for the experimental processes. For further GC analysis, standard alkene and alkane solutions ranging from C₈ to C₂₀, along with the internal standard 1-bromohexane, were purchased from Sigma-Aldrich and used without any additional purification steps. The feedstock for this process consisted of fats, oils, and grease (FOG), which were collected from the Seri Kembangan Indah Water treatment plant in Malaysia.

Catalyst preparation

The electrodeposition process was carried out with Pt serving as the counter electrode, while Fe foam was used as the working electrode. Both electrodes were submerged in an electrolytic solution containing Ni(NO₃)₂·6H₂O at a concentration of 0.34 M, along with Ce(SO₄)₂ at varying concentrations of 0.30 M and 0.42 M. The electrodeposition was performed at a voltage of 2.5 V for 30 min. After electrodeposition, the Fe foam coated with Ni and Ce was thoroughly washed with deionized water and then dried. The resulting catalyst was labeled as Ni_aCe_b/FeF, in which a 0.34M and b 0.30M, with a concentration of 0.34M

and b = 0.30M or 0.42M. The catalysts produced were designated as Fe-F, $Ni_{0.34}Ce_{0.30}/Fe$ -F and $Ni_{0.34}Ce_{0.42}/Fe$ -F.

Catalyst characterization

X-ray diffraction (XRD) analysis, using a Shimadzu XRD-6000 instrument (Japan), was performed to investigate the crystallinity and identify the phases present in the catalysts. The instrument operated with a scan speed of 4°C per minute over a 2θ range of 5° to 40°. The crystallite size was determined using Debye-Scherrer's equation. Then, field-emission scanning electron microscopy (FESEM) was applied to observe the porous structure of the Fe foam and its morphology. To evaluate the surface area, the Brunauer-Emmet-Teller (BET) method employed, using an N₂ adsorption/desorption analyzer (Sorpmatic 1990 series, Thermo-Finnegan, USA). The acidic and basic properties of the catalysts were analyzed using ammonia temperature-programmed desorption (NH3-TPD) with a Thermo-Finnigan TPDRO 1100 (USA) instrument.

Hydrodeoxygenation of FOG

The hydrodeoxygenation (HDO) study was conducted on fats, oils, and grease (FOG) in a 300 mL custombuilt stainless steel batch reactor. 10g of FOG and 1 cm² of Fe-F catalyst into the reactor. This was followed by purging high-purity hydrogen (H₂) gas N₂. The pressure inside the reactor was then adjusted to 5 MPa. Subsequently, the reactor was heated to 400°C while stirring at 200 rpm for 6 h. The steps were repeated for the $Ni_{0.34}Ce_{0.30}/Fe-F$ and $Ni_{0.34}Ce_{0.42}/Fe-Fe-Fe$ F. For the liquid analysis, GC-FID analysis provided detailed data on both the hydrocarbon yield and the selectivity of the hydrocarbon products analyzed using gas chromatography (GC) with flame ionization detection (FID) (Agilent 7890A series, USA)(HP-5 capillary column (30 m in length, 0.32 mm inner diameter, and a film temperature of 300°C) and a GCmass spectrometer (GCMS) (SHIMADZU QP2010) was used to Isolate complex mixtures, measure analyte concentrations, recognize unidentified peaks, and detect trace contaminants.

Results and Discussion Catalysts screening

The XRD patterns for Fe-F, $Ni_{0.34}Ce_{0.30}/Fe$ -F and $Ni_{0.34}Ce_{0.42}/Fe$ -F catalysts were shown in **Figure 1**. The results indicated that the Fe-F catalyst showed a high peak at 20 value of 45.0°, corresponding to the presence of an iron metallic peak. In some studies, the XRD pattern of iron shows a big peak near 44.6°, which is attributed to the (110) reflection of BCC iron [27]. The same observations were noted on the other catalysts because all of them had Fe-Foam as their support. Furthermore, the XRD patterns of Ni (a = 0.34 M) and Ce (x = 0.30 M and 0.42 M) showed

features at 2θ values of 45.0° , 78.4° (ICDD card: 00-001-1266), and 66.2° (ICDD card: 00-033-0323), which symbolize the metallic phase for Ni and Ce metals. Metal oxide also shows up at the peak of $2\theta = 36.2^{\circ}$, 38.7° and 44.0° for the oxide formation of Ce, Fe and Ni.

The Ni_{0.34}Ce_{0.42}/Fe-F catalyst with the higher cerium content shows more intense Ce-related peaks. It presents a slight decrease in the relative intensity of Fe peaks in comparison with the lower cerium content catalyst, indicating that higher cerium loading influences the Fe crystalline structure and possibly forms more Ce₂O₃ phase at the expense of metallic phases [28] Catalyst crystallite size was calculated from the line broadening XRD patterns of the intense 2θ=45.0° using Scherrer's equation with the value ranging 33.6 – 89.0 nm. Indeed, the addition of cerium leads to a broadening of the Fe peak, thus decreasing the intensity of the Fe peak, and finally lowers the Fe crystallite size. These results are consistent with previous reports in which excess cerium causes lattice strain, causing other metal peaks in the XRD pattern to broaden [29,30]. Collectively, these XRD peaks confirmed the successful loading of nickel and cerium species on the iron foam surface.

Figure 2(a) shows the acidity profiles of the catalysts evaluated by temperature-programmed desorption of NH₃. TPD-NH₃ profiles for Ni_{0.34}Ce_{0.30}/Fe-F showed NH₃ desorption peaks of 122 μmolg⁻¹ at temperatures between 200-500 °C, suggesting that the catalyst possessed medium acid sites. For Ni_{0.34}Ce_{0.42}/Fe-F, the catalyst shows weak acid strength (50-200°C) and possesses a broader desorption peak between 300-550°C, which falls in the range of the medium acid profile (200-600°C). The catalyst, however, exhibited a higher acidity value of 233 μmolg⁻¹ compared to Ni_{0.34}Ce_{0.30}/Fe-F. Therefore, it is worth noting that with an increase in the quantity of cerium deposited on the catalyst, the catalyst's acidity increases as well, as presented in **Table 1**.

Indeed, the redox behavior of cerium influences the catalyst's surface properties, which consequently affects its acidity [31,32]. Worth noting to mention, weak to medium acidic sites play an important role in oxygenated species removal, while strong acidic sites are efficient at cracking reaction catalysis and dehydrogenation [33]. Due to its acidity nature, the modified Fe-F catalyst is believed to show outstanding HDO activity. For Fe-F, the Fe-F doesn't portray any broad high peaks and has a low acidic value of 76 µmolg⁻¹. The Fe-F low acidity is attributed to the lack of promoters Ni or Ce and the nature of the iron species, which Fe³⁺ cations have weak acidity [34,35]. Based on these results, it is believed that Fe-F demonstrates poor HDO activity.

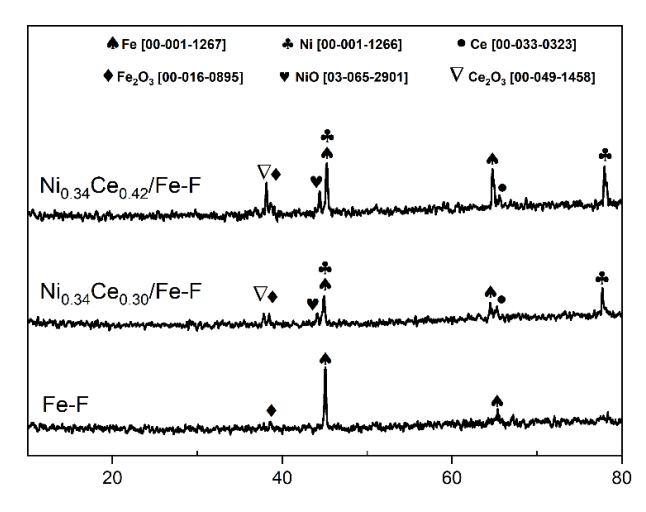


Figure 1. XRD analysis of Fe-F, Ni_{0.34}Ce_{0.30}/Fe-F and Ni_{0.34}Ce_{0.42}/Fe-F

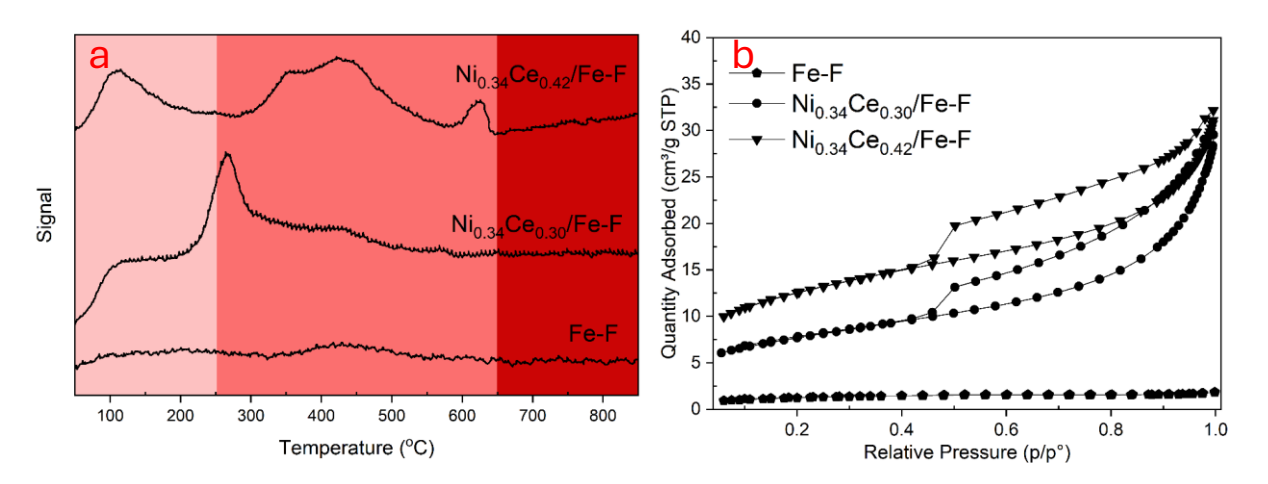


Figure 2. (a) TPD-NH₃ analysis of the catalysts and (b) BET adsorption-desorption analysis of the catalysts

Table 1. Physiochemical properties of Fe-F, Ni_{0.34}Ce_{0.30}/Fe-F and Ni_{0.34}Ce_{0.42}/Fe-F

Catalyst	Crystallite Size (nm)	BET Surface Area (m²/g)	Average Pore Diameter (nm)	Acid strength (μmolg ⁻¹)	
				Weak +	Strong
				medium acid	acid
Fe-F	33.6	4.45	2.31	76	-
$Ni_{0.34}Ce_{0.30}/Fe-F$	89.0	27.59	4.83	122	-
Ni _{0.34} Ce _{0.42} /Fe-F	68.7	45.13	3.50	233	-

The information in **Figure 2(b)** presented the BET adsorption-desorption analysis of the catalyst. For the graph, the catalyst displays the Type IV isotherm and demonstrates the mesoporous nature of materials with well-defined mesopore structures [36,37]. However, it is only applicable for Ni_{0.34}Ce_{0.30}/Fe-F and Ni_{0.34}Ce_{0.42}/Fe-F. As seen in **Table 1** comparing the BET surface area of Fe-F, Ni_{0.34}Ce_{0.30}/Fe-F and Ni_{0.34}Ce_{0.42}/Fe-F, the specific BET surface area

increases as the presence of cerium is increased. The trend rises from 4.45 m²/g for Fe-F to 27.59 m²/g and 45.13 m²/g for Ni_{0.34}Ce_{0.30}/Fe-F and Ni_{0.34}Ce_{0.42}/Fe-F, respectively, with higher values. Even though the surface area increases for the catalyst, the average pore diameter of the catalyst exhibits an up-and-down trend. As presented in **Table 1**, the value reduces from 4.83 nm to 3.5 nm for the deposited catalysts. This can occur due to the amount of cerium that occupied the

pore of the Fe foam. These results are comparable with a previous study, whereby the specific BET surface area drastically dropped after the impregnation of Co and W species onto the SA support [38]. This shows that the deposition of active metal species onto the catalyst support can affect the pore structure of the catalyst and hence its specific BET surface area. The doping of these metals might also trigger oxidation processes, which can further modify the surface characteristics of the catalyst [39].

Figure 3a-b shows the morphological analysis study of Fe-F and Ni_{0.34}Ce_{0.42}/Fe-F. Before the modification of Fe-F, the Fe-F shows the presence of pores, validating the porous structure nature of the Fe-F itself (Figure 3a). Meanwhile, during the time of deposition of Ni and Ce, the morphology changes and becomes a porous needle structure, as shown in Figure 3b. Apparently, the porous needle-like structure allows alternative pathways for reactants to access active sites, hence circumventing diffusional limitations typically excluding catalytic activity [40]. Based on EDX mapping analysis, the results indicated that nickel and cerium homogeneously distributed over the surface of the iron foam support. It has been suggested in earlier research that this may enhance the catalytic HDO activity [41].

Catalytic activity in HDO

Hydrodeoxygenation (HDO) of FOG was investigated by employing metal-modified catalysts in different reaction conditions in a purposely designed stainlesssteel reactor. Moreover, the effect of Ce concentrations on the HDO process was also investigated further. Parameters such as pressure, reaction time, and temperature were kept at 5 MPa for 6 hours at 400°C. The reaction parameters employed in this work were chosen based on the optimum HDO conditions in other studies [42-46]. GC-FID and GC-MS analysis indicated that both saturated and unsaturated hydrocarbon fractions were present in the HDO liquid products with carbon chain lengths between C₈ and C₂₀ (Figure 4a-c). It is important to note that a control experiment was also performed under the same reaction conditions and parameters, but in the absence of a catalyst, for comparison. The results indicate that the lowest hydrocarbon yield, 7.5%, was achieved for the blank experiment (Figure 4a). By comparison, reactions involving catalysts under the same conditions show considerable improvements over the blank reaction, yielding hydrocarbons in the range 53–74%, clearly indicating the occurrence of catalytic HDO. Specifically, Fe-F, 57% hydrocarbon yield, Ni_{0.34}Ce_{0.30}/Fe-F (74%), whereas the Ni_{0.34}Ce_{0.42}/Fe-F catalyst yielded 53% hydrocarbon yield. Importantly, the addition of Ni and Ce on Fe foam leads to an increase in active sites for hydrogen activation and hydrogenation reactions. Indeed, Ni facilitates H-H cleavage, whereas Ce generates oxygen vacancies that help in breaking C-O bonds [47,48], remarkably increasing the HDO activity and leading to hydrocarbon yields of over 50%. However, the HDO activity declines with the addition of 0.42 M Ce, which implicates that excess Ce species mask the Ni active sites, thus reducing H-H cleavage activity [49–51]. All these results together signify that an optimum quantity of Ni and Ce is required for inducing high C-O and H-H cleave activity, thus improving the HDO of FOG and subsequently producing hydrocarbons mainly in the range of C₁₅-C₁₈. Interesting to note that, FOG contains mainly palmitic acid (C16:0) and oleic acid (C18:1), however result demonstrated that the hydrocarbon distribution mainly in range of n-(C₁₀-C₁₅ and C₁₇) (Figure 4b). This wide distribution further implicated that the catalyst also found effective for cracking activity, thus producing lighter hydrocarbons and gases [44,52]. An earlier study also implicated that high temperature may initiate the thermal cracking of longer hydrocarbon chains, especially when the reaction duration is prolonged [44]. At such high temperatures, thermal cracking can take place, leading to the breakdown of longer hydrocarbon chains into shorter ones, which may affect product distribution and yield. However, it is interesting to note here that hydrocarbon selectivity within the desired range $(n-(C_{15}-C_{18}))$ is still achievable (60-74%), inducing only modest cracking, which occurs without significantly affecting overall fuel quality.

Besides that, GCMS analysis (Figure 4c) depicts the mass fraction profile of the HDO product. Indeed, evident formation of aldehyde such as Octadecanal, alcohol such as 1-Hexadecanol (C₁₆H₃₄O), 9-Octadecanol (C₁₈H₃₈O), 1-Heptadecanol (C₁₇H₃₆O), 1-Pentadecanol (C₁₅H₃₂O), and carboxylic acid such as n-Hexadecanoic Acid (C₁₆H₃₂O₂), n-Octadecanoic Acid (C₁₈H₃₆O₂), Pentadecanoic Acid (C₁₅H₃₀O₂) were identified in the liquid product. This may be due to secondary reaction during HDO of FOG. Figure 5 presented the suggested reaction routes for HDO of FOG. According to the GC-MS analysis, it is suggested that HDO of FOG takes place through direct hydrodeoxygenation and secondary reaction route. In direct hydrodeoxygenation (Route 1), carboxylic acids are transformed into saturated hydrocarbons, whereas in the secondary reaction (Route 2), carboxylic acids are partially transformed into aldehydes and alcohols. The blank and catalytic reactions showed a notable discrepancy, indicating the vital role of the catalyst in inducing selective HDO activity. Interestingly, the quantity of saturated hydrocarbon chain of HDO when Ni_{0.34}Ce_{0.42}/Fe-F catalyst is considerably higher in comparison to Ni_{0.34}Ce_{0.30}/Fe-F. This implies that with

increased cerium content, the hydrogenation activity is enhanced, more efficient HDO routes are facilitated, and greater quantities of saturated hydrocarbons are produced though not as high as that obtained using Ni-

rich catalysts. Thus, the cerium content still needs to be cautiously controlled and means to improve the effectiveness of Ce should be explored.

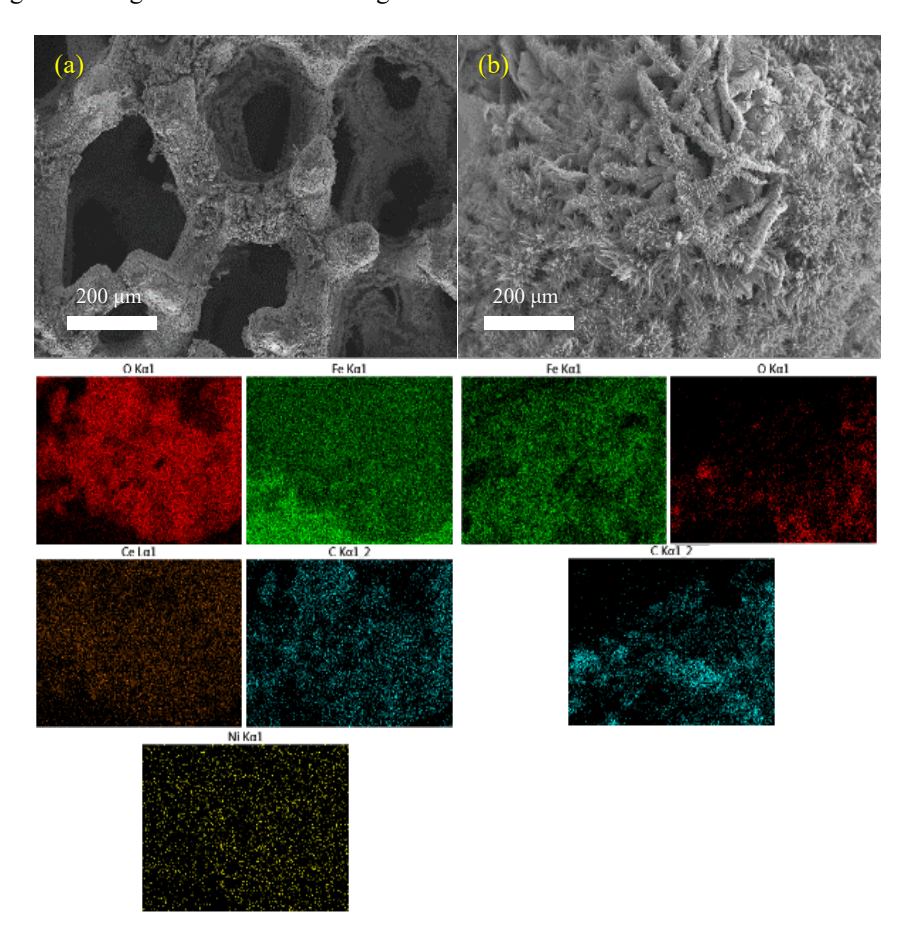


Figure 3. FESEM-EDX analysis of (a) Fe-F and (b) Ni_{0.34}Ce_{0.42}/Fe-F

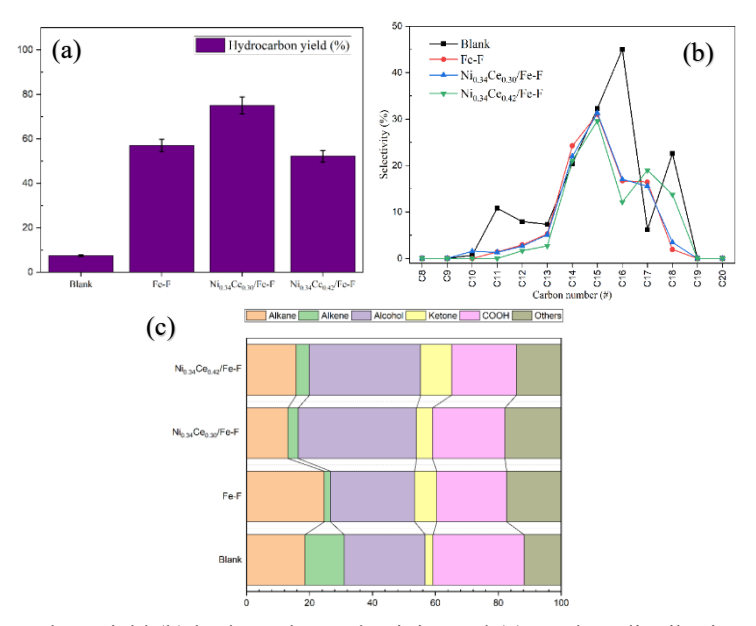


Figure 4. (a) Hydrocarbon yield (b) hydrocarbon selectivity and (c) product distribution after HDO reaction

Pathway 1: Direct Hydrodeoxygenation

$$O$$
 + $2H_2$ \longrightarrow R OH + H_2O \longrightarrow R $-CH_3$ + H_2O (Hydrodeoxygenation)

Pathway 2: Intermediate Formation

Figure 5. Reaction pathways of hydrodeoxygenation

Conclusions

In this study, Ni and Ce-added Fe foam catalysts were prepared by means of an electrodeposition process. The catalysts proved to be highly effective in the production of diesel-type hydrocarbons from oleic acid and palmitic acid in a composition predominantly of FOG with product selectivity ranging from 66% to 71% and conversions ranging from 53% to 74%. High activity for hydrodeoxygenation is positively influenced by Ce and Ni loading over the support, with product distribution more in the direction of saturated hydrocarbons and n-(C₁₅+C₁₇) and n-(C₁₆+C₁₈) selective. Also, the acidity sites improve HDO activity mostly due to favouring the formation of carbocations; thus, with a higher value of weak to medium acidic sites, it favours the catalyst. The highest Ce loading content used in the catalyst, Ni_{0.34}Ce_{0.42}/Fe-F, showed the best catalytic activity in the HDO reaction because 0.42 M is the optimal concentration with 0.34 M Ni. Higher Ce species will cause a reduction in H-H bonding cleavage activity due to the blockage of active sites of Ni. Overall, enough Ni and Ce is needed to increase the high C-O and H-H cleave activity, thereby enhancing the HDO of FOG.

Acknowledgement

The authors would like to express their gratitude to the Ministry of Higher Education (MOHE) Malaysia for the provision of financial support to this research work via the Fundamental Research Grant Scheme (FRGS/1/2023/STG04/UKM/02/6), Dana Impak Perdana 2.0 (DIP-2024-027), Geran Translasi UKM (UKM-TR2024-15), and Universiti Kebangsaan Malaysia (UKM) and Universiti Kebangsaan Malaysia (UPM) for the laboratory facilities.

References

- 1. Fossil fuel use reaches global record despite clean energy growth. Access from https://www.theguardian.com/environment/arti cle/2024/jun/20/fossil-fuel-use-reaches-global-record-despite-clean-energy-growth (accessed September 19, 2024).
- 2. Executive Summary CO₂ Emissions in 2023 analysis. Access from https://www.iea.org/reports/co2-emissions-in-2023/executive-summary (accessed September 19, 2024).
- 3. Rashid U, Lee CL, Hazmi B, Gamal S, and Beygisangchin M. (2024). Standard specifications for renewable diesel. *Renewable Diesel: Value Chain, Sustainability, and Challenges*, 2024:33–63.
- 4. Vignesh P, Pradeep Kumar AR, Ganesh NS, Jayaseelan V, and Sudhakar K. (2021). Biodiesel and green diesel generation: an overview. Oil & Gas Science and Technology Revue d'IFP Energies Nouvelles,76:6.
- 5. Riazi B, Mosby JM, Millet B, and Spatari S. (2020). Renewable diesel from oils and animal fat waste: implications of feedstock, technology, co-products and ILUC on life cycle GWP. Resource Conservation Recycling 2020;161:104944.
- Asikin-Mijan N, Juan JC, Taufiq-Yap YH, Ong HC, Lin YC, AbdulKareem-Alsultan G, et al. (2023). Towards sustainable green diesel fuel production: Advancements and opportunities in acid-base catalyzed H₂-free deoxygenation process. *Catalysis Communication*, 182:106741.
- 7. Sultana N, Roddick FA, Pramanik BK. (2024). Fat, oil and grease wastewater and dishwashers: Uncovering the link to FOG deposition. *Science of the Total Environment*, 907:168032.

- 8. Wallace T, Gibbons D, O'Dwyer M, Curran TP. (2017). International evolution of fat, oil and grease (FOG) waste management A review. *Journal Environmental Management*, 187:424–35
- 9. Yusuf HH, Roddick F, Jegatheesan V, Gao L, and Pramanik BK. (2023). Tackling fat, oil, and grease (FOG) build-up in sewers: Insights into deposit formation and sustainable in-sewer management techniques. *Science of the Total Environment*, 904:166761.
- 10. Taipabu MI, Viswanathan K, Wu W, and Nagy ZK. (2021). Production of renewable fuels and chemicals from fats, oils, and grease (FOG) using homogeneous and heterogeneous catalysts: Design, validation, and optimization. *Chemical Engineering Journal*, 424:130199.
- 11. Abomohra AEF, Elsayed M, Esakkimuthu S, El-Sheekh M, and Hanelt D. (2020). Potential of fat, oil and grease (FOG) for biodiesel production: A critical review on the recent progress and future perspectives. *Progress Energy Combustion Sciences*, 81:100868.
- 12. Vastolo A, Riedmüller J, Cutrignelli MI, and Zentek J. (2022). Evaluation of the effect of different dietary lipid sources on dogs' faecal microbial population and activities. *Animals* (Basel), 12: 111368.
- 13. Ahmed RA, and Huddersman K. (2023). Short review of biodiesel production by the esterification/transesterification of wastewater containing fats oils and grease (FOGs). Energy and Sustainable Futures: Proceedings of the 3rd ICESF, 2023: 285-299.
- 14. Ruangudomsakul M, Osakoo N, Wittayakun J, Keawkumay C, Butburee T, and Youngjan S, et al. (2022). Hydrodeoxygenation of palm oil to green diesel products on mixed-phase nickel phosphides. *Molecular Catalysis*, 523:111422.
- 15. He Z, and Wang X. (2013). Hydrodeoxygenation of model compounds and catalytic systems for pyrolysis bio-oils upgrading. *Catalysis for Sustainable Energy* 2013:1.
- 16. Attia M, Farag S, and Chaouki J. (2020). Upgrading of oils from biomass and waste: catalytic hydrodeoxygenation. *Catalysts*, 10:1381.
- 17. Ojagh H. (2020). Hydrodeoxygenation (HDO) catalysts characterization, reaction and deactivation studies. Thesis of Doctor Philosophy.
- 18. Klaewkla R, Arend M, F. W. (2011). A review of mass transfer controlling the reaction rate in heterogeneous catalytic systems. *Mass Transfer Advanced Aspects*, 2011: 22962.
- 19. Tran N, Uemura Y, Trinh T, and Ramli A. (2021). Hydrodeoxygenation of guaiacol over

- Pd-Co and Pd-Fe catalysts. *Deactivation and Regeneration Processes*, 9:430.
- 20. Yan P, Li MMJ, Kennedy E, Adesina A, Zhao G, and Setiawan A, et al. (2020). The role of acid and metal sites in hydrodeoxygenation of guaiacol over Ni/Beta catalysts. *Catalysis Science Technology*, 10: 810-825.
- 21. Chen TS, Guo L, Peng HW, Li YQ, Wang XB, and Bai HC, et al. (2022). Tuning support acidity of Ni-based catalysts to improve hydrodeoxygenation activity for dibenzofuran. *Fuel Processing Technology*, 236:107440.
- 22. Zhang, Y., Liu, T., Xia, Q., Jia, H., Hong, X., & Liu, G. (2021). Tailoring of surface acidic sites in Co–MoS2 catalysts for hydrodeoxygenation reaction. *The Journal of Physical Chemistry Letters*, 12(24): 5668-5674.
- Jiang S, Ji N, Diao X, Li H, Rong Y, and Lei Y, et al. (2021). Vacancy engineering in transition metal sulfide and oxide catalysts for hydrodeoxygenation of lignin-derived oxygenates. *ChemSusChem*, 14: 4377-4396.
- Schimming SM, Lamont OD, König M, Rogers AK, D'Amico AD, and Yung MM, et al. (2015). Hydrodeoxygenation of guaiacol over ceria– zirconia catalysts. *ChemSusChem*, 8:2073-283.
- Resende KA, Braga AH, Noronha FB, and Hori CE (2019). Hydrodeoxygenation of phenol over Ni/Ce1-xNbxO₂ catalysts. *Applied Catalyst B*, 245:100-113.
- 26. Ali H, Vandevyvere T, Lauwaert J, Kansal SK, Saravanamurugan S, and Thybaut JW. (2022). Impact of oxygen vacancies in Ni supported mixed oxide catalysts on anisole hydrodeoxygenation. *Catalyst Communication*, 164:106436.
- 27. Dalshad Omar H. (2015). Investigation the structure and morphology of iron metallic by difference techniques. *Journal of Nano Advances Materials*, 3:57.
- 28. Zhang F., Yao S., Liu Z., Gutiérrez R. A., Vovchok D., Cen J., ... and Rodriguez, J. A. (2018). Reaction of methane with MOx/CeO₂ (M= Fe, Ni, and Cu) catalysts: In situ studies with time-resolved X-ray diffraction. *The Journal of Physical Chemistry C*, 122(50): 28739-28747.
- Holder CF, and Schaak RE. (2019). Tutorial on powder X-ray diffraction for characterizing nanoscale materials. ACS Nano, 13: 7359-7365.
- 30. Laguna O. H., Centeno M. A., Boutonnet M., and Odriozola, J. A. (2011). Fe-doped ceria solids synthesized by the microemulsion method for CO oxidation reactions. *Applied Catalysis B: Environmental*, 106(3-4): 621-629
- 31. Gao S, Yu D, Zhou S, Zhang C, Wang L, Fan X, et al. (2023). Construction of cerium-based

- oxide catalysts with abundant defects/vacancies and their application to catalytic elimination of air pollutants. *Journal of Material Chemistry A*, 11: 19210-19243.
- 32. Cai M, Bian X, Xie F, Wu W, Cen P. (2021). Preparation and performance of cerium-based catalysts for selective catalytic reduction of nitrogen oxides: A critical review. *Catalysts*, 11: 1-23.
- 33. Wang H, Lin H, Feng P, Han X, and Zheng Y. (2017). Integration of catalytic cracking and hydrotreating technology for triglyceride deoxygenation. *Catalyst Today*, 291: 172-179.
- 34. Wu Y, Pei C, Tian H, Liu T, Zhang X, Chen S, et al. (2021). Role of Fe species of Ni-based catalysts for efficient low-temperature ethanol steam reforming. *Journal of American Chemical Society*, 1: 1459-1470.
- 35. Wang Y, Yan N, and Chen Z. (2024). Identification of coke species on Fe/USY catalysts used for recycling polyethylene into fuels. *RSC Advances*, 14: 22056-22062.
- 36. Ali NS, Harharah HN, Salih IK, Cata Saady NM, Zendehboudi S, and Albayati TM. (2023) Applying MCM-48 mesoporous material, equilibrium, isotherm, and mechanism for the effective adsorption of 4-nitroaniline from wastewater. *Scientific Report*, 2023:13.
- 37. Sotomayor, F. J., Cychosz, K. A., and Thommes, M. (2018). Characterization of micro/mesoporous materials by physisorption: concepts and case studies. *Accounts Materials Surface Research*, 3(2): 34-50.
- 38. Asikin-Mijan N, AbdulKareem-Alsultan G, Mastuli MS, Salmiaton A, Azuwa Mohamed M, Lee H V., et al. (2022). Single-step catalytic deoxygenation-cracking of tung oil to bio-jet fuel over CoW/silica-alumina catalysts. *Fuel*, 2022: 325.
- Pawelec B, Mariscal R, Fierro JLG, Greenwood A, and Vasudevan PT. (2001). Carbonsupported tungsten and nickel catalysts for hydrodesulfurization and hydrogenation reactions. Applied Catalysis A General, 206: 295-307.
- 40. Peng P, Gao XH, Yan ZF, and Mintova S. (2020). Diffusion and catalyst efficiency in hierarchical zeolite catalysts. *National Science Review*, 7: 1726-1742.
- 41. Savannah River National Laboratory (2025). Savannah Highly Dispersed Metal Catalyst Access from https://www.srnl.gov/tech_briefs/highly-dispersed-metal-catalyst/ [Accessed June 25, 2025].
- 42. Ojagh Houman. Hydrodeoxygenation (HDO) catalysts: characterization, reaction and deactivation studies. Chalmers University of Technology; 2018.

- 43. Olbrich W, Boscagli C, Raffelt K, Zang H, Dahmen N, and Sauer J. (2016). Catalytic hydrodeoxygenation of pyrolysis oil over nickel-based catalysts under H₂/CO₂ atmosphere. Sustainable Chemical Processes, 2016 4:1-8.
- 44. BiLge S, Donar YO, Ergenekon S, Özoylumlu B, and Sinağ A. (2023). Green catalyst for clean fuel production via hydrodeoxygenation. *Turkish Journal Chemistry*, 47: 968.
- 45. Nur Azreena I, Lau HLN, Asikin-Mijan N, Hassan MA, Izham SM, and Safa Gamal M, et al. (2022). Hydrodeoxygenation of fatty acid over La-modified HZSM5 for premium quality renewable diesel production. *Journal of Analysis and Applied Pyrolysis*, 2022: 161.
- 46. Chang H, Abdulkareem-Alsultan G, Taufiq-Yap YH, Mohd Izham S, and Sivasangar S. (2024) Development of porous MIL-101 derived catalyst application for green diesel production. *Fuel*, 355:129459.
- 47. Kim M, Tomechko M, and Zhai S. (2025). Nickel-catalyzed simultaneous iron and cerium redox reactions for durable chemical looping dry reforming of methane. *Journal of Materials Chemistry A*, 13: 20942-20954
- Jin W., Pastor-Pérez L., Villora-Picó J. J., Sepúlveda-Escribano A., Gu S., and Reina T. R. (2019). Investigating new routes for biomass upgrading: "H₂-free" hydrodeoxygenation using Ni-based catalysts. ACS Sustainable Chemistry & Engineering, 7(19): 16041-16049.
- 49. Dzakaria N., Lahuri A. H., Saharuddin T. S. T., Samsuri A., Salleh F., Isahak, W. N. R. W., ... and Yarmo M. A. (2021). Preparation of cerium doped nickel oxide for lower reduction temperature in carbon monoxide atmosphere. *Malaysian Journal of Analytical Sciences*, 25(3): 521-531.
- Viscardi R, Barbarossa V, Gattia DM, Maggi R, Maestri G, and Pancrazzi F. (2020). Effect of surface acidity on the catalytic activity and deactivation of supported sulfonic acids during dehydration of methanol to DME. New Journal of Chemistry, 44:16810-16820.
- 51. Oh M, Jin M, Lee K, Kim JC, Ryoo R, and Choi M. (2022). Importance of pore size and Lewis acidity of Pt/Al₂O₃ for mitigating mass transfer limitation and catalyst fouling in triglyceride deoxygenation. *Chemical Engineering Journal*, 439:135530.
- 52. Si Z, Zhang X, Wang C, Ma L, Dong R. (2017). An overview on catalytic hydrodeoxygenation of pyrolysis oil and its model compounds. *Catalysts*, 2017: 7.